Optica Applicata, Vol. XIV, No. 3, 1984

Numerical investigation of the two-point resolution in the holographic imaging*

Jerzy Nowak, Marek Zając

Institute of Physics, Technical University of Wrocław, Wybrzeże Wyspiańskiego 27, 50-370 Wrocław, Poland.

In this paper a numerical algorithm enabling the calculation of the light intensity distribution in the holographic image of a two-point objects is presented. After testing its accuracy it was used to evaluate the images of two-point objects obtained in holographic imaging with aberrations. Based on the results obtained the influence of aberrations on the two-point resolution was analysed, depending on the field angle and aperture of hologram.

1. Principle of method

Typical investigation of the imaging quality for classical optical system or for a hologram consists usually in the analysis of the image of a point object. Imaging quality can be described also by stating the wave aberration, calculating the aberration coefficients or by analysing the light energy distribution in an aberration spot [1–3]. In the latter case there is a difference between the possibilities of the image quality evaluation for the coherent and incoherent illumination. For the incoherent case the light energy distribution can be calculated by a *spot diagram* method. For the coherent-case, however, a geometric method of the aberration spot estimation is inadequate. It can give only very general outlook of the approximate shape of the spot, but it does not provide any information about the light energy distribution inside it.

In the papers [4, 5] the authors have proposed a numerical method for calculation of this distribution in the case of holographic imaging. It is well known, however, that in coherent illumination (and this is a typical case in holography) the conclusions drawn from the analysis of the image of a point cannot be directly extended for the case of a many-point object. Therefore individual calculations are necessary for this case.

The present paper is devoted to the investigations of the two-point object imaging which enables us to estimate the two-point resolution limit and to determine the influence of aberrations on its value in holographic imaging.

---

* This paper has been prepared under the Research Project M. R. I.5, and was presented in the European Optical Conference (EOC'83) held in Rydzyna, May 30–June 4, 1983.

Schematic diagram of the hologram recording and image reconstruction geometries is presented in Fig. 1. In the hologram plane three waves interfere:

$$
\begin{aligned}
U_1 &= A_1 e^{i\varphi_1},\\
U_2 &= A_2 e^{i\varphi_2},\\
U_R &= A_R e^{i\varphi_R}
\end{aligned}
\tag{1}
$$

where: $\varphi_1 = k_1 R_1$, $\varphi_2 = k_1 R_2$, $\varphi_R = k_1 R_R$, $k_1 = 2\pi/\lambda_1$ (R_1, R_2, R_R denote the distances from one of the object wave sources or the reference wave source to the chosen point on a hologram, respectively, λ_1 is a wavelength of light used when recording a hologram).

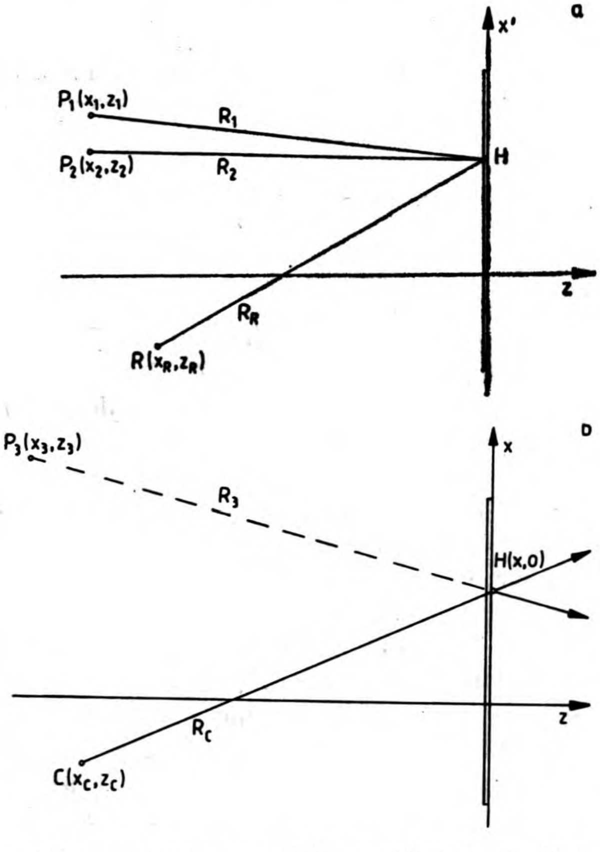

Fig. 1. Scheme of the holographic recording (a) and reconstruction (b) geometries

If we assume, as it is usually done, that

$$A_1 = A_2 = A_R = 1, \tag{2}$$

then the light intensity distribution in the hologram plane would be given by the formula

$$
\begin{aligned}
I' = 3 &+ 2\left[e^{ik_1(R_1-R_2)} + e^{ik_1(R_2-R_1)}\right] + 2\left[e^{ik_1(R_1-R_R)} + e^{ik_1(R_R-R_1)} + e^{ik_1(R_2-R_R)}\right.\\
&\left.+ e^{ik_1(R_R-R_2)}\right].
\end{aligned}
\tag{3}
$$

The first term describes a constant background, so it does not contribute any useful information, hence it can be neglected.

In this case, and under the assumption of linear recording, an amplitude transmittance of a hologram can be expressed by

$$t = e^{ik_1(R_1-R_R)}+e^{ik_1(R_R-R_1)}+e^{ik_1(R_2-R_R)}+e^{ik_1(R_R-R_2)}. \tag{4}$$

Now, let a reconstructing wave originating from a point source placed in the point C fall on a hologram (Fig. 1b)

$$U_C = A_C e^{i\varphi_C} \tag{5}$$

where: $\varphi_C = k_2 R_C$, $k_2 = 2\pi/\lambda_2$, $A_C = 1$, (R_C denotes a distance from the point C to the chosen point on a hologram, λ_2 is a wavelength of light used for image reconstruction).

On its way from the hologram to image the wave phase changes additionally by $\varphi_3 = k_2 R_3$ (R_3 being the distance between the point on the hologram and the point in a plane in which the image is observed). Finally, the wave reaching the considered image point can be described as follows:

$$\begin{aligned}U_3 = {} & e^{ik_2(\mu R_1-\mu R_R+R_C+R_3)}+e^{ik_2(\mu R_R-\mu R_1+R_C+R_3)}+e^{ik_2(\mu R_2-\mu R_R+R_C+R_3)} \\ & +e^{ik_2(\mu R_R-\mu R_2+R_C+R_3)}\end{aligned} \tag{6}$$

where $\mu = \lambda_2/\lambda_1$.

The considerations we have been carrying on till now refer to only one *ray*. To find the light intensity in a given image point it is necessary to take into account contributions from all interfering *rays*:

$$I_3'' = \left|\sum_{i=1}^{n_x}\sum_{j=1}^{n_y} U_{3\,i,j}\right|^2 \tag{7}$$

where $i = 1, \ldots, n_x$, $j = 1, \ldots, n_y$ number the summed *rays*. The manner in which the *rays* are selected as well as the choice of its number and density have been described in the papers [4, 5] and will not be repeated here.

Finally the light intensity distribution in a given point is expressed by a formula

$$\begin{aligned}I_3'' = {} & \left[\sum_{i=1}^{n_x}\sum_{j=1}^{n_y}(\cos A_{i,j}+\cos B_{i,j}+\cos C_{i,j}+\cos D_{i,j})\right]^2 \\ & +\left[\sum_{i=1}^{n_x}\sum_{j=1}^{n_y}(\sin A_{i,j}+\sin B_{i,j}+\sin C_{i,j}+\sin D_{i,j})\right]^2\end{aligned} \tag{8}$$

where:

$$\begin{aligned}A_{i,j} &= k_2(\mu R_{1\,i,j}-\mu R_{R\,i,j}+R_{C\,i,j}+R_{3\,i,j}),\\ B_{i,j} &= k_2(\mu R_{R\,i,j}-\mu R_{1\,i,j}+R_{C\,i,j}+R_{3\,i,j}),\\ C_{i,j} &= k_2(\mu R_{2\,i,j}-\mu R_{R\,i,j}+R_{C\,i,j}+R_{3\,i,j}),\\ D_{i,j} &= k_2(\mu R_{R\,i,j}-\mu R_{2\,i,j}+R_{C\,i,j}+R_{3\,i,j}).\end{aligned}$$

However, to make the results independent of the number of *rays* taken into account it is necessary to perform a normalization, as in papers [4, 5]

$$I_3 = \frac{I_3''}{(n_x n_y)^2}. \tag{9}$$

2. Numerical results

The presented above method of the light intensity evaluation in the holographic image of the two-point objects should be tested in order to establish the accuracy calculations. The easiest way to do it is to analyse an aberration-free imaging. The recording and reconstruction geometries are shown in Fig. 2. For shorten-

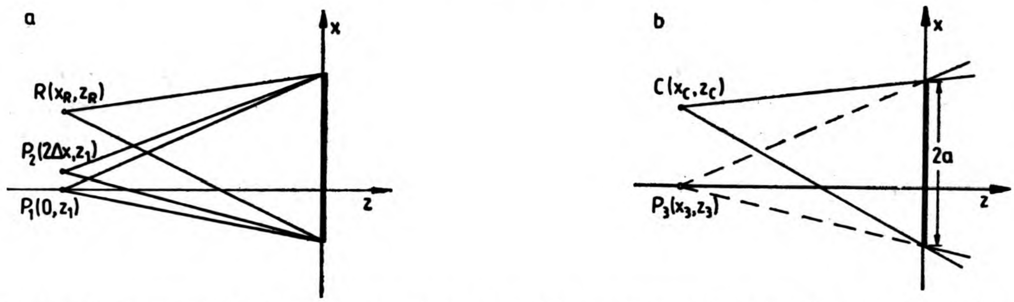

Fig. 2. Geometry of hologram recording (a) and image reconstruction (b) used for testing the algorithm:
$x_1 = 0$, $x_2 = 2\Delta x$, $x_R = 5$ mm, $x_C = 5$ mm,
$z_1 = -100$ mm, $z_2 = -100$ mm, $z_R = -100$ mm, $z_C = -100$ mm,
$m = \mu = 1$, $2a = 2$ mm, $\lambda_2 = 0.0006328$ mm, $z_3 = -100$ mm

ing the computing time we have restricted ourselves to a simplified case of one-dimensional hologram and calculated the light intensity distribution in an image of the two-point object for several distances between the object points. The theoretical function describing this dependence is as follows:

$$I = \left| \operatorname{sinc}\left(\frac{2\pi a x_3}{\lambda_2 z_3}\right) + \operatorname{sinc}\left(\frac{2\pi a (x_3 - 2\Delta x)}{\lambda_2 z_3}\right) \right|^2. \tag{10}$$

The curves drawn in heavy lines in Fig. 3 illustrate this distribution, while the values calculated according to our algorithm are marked by circles. It may be seen that the consistence is very good.

To investigate the influence of aberrations on the resolution the calculations were made for a selected case of holographic recording and image reconstruction. The reconstruction geometry was chosen in such a way that the image was emphatically aberrated. The numerical data referring to this case are marked in Fig. 4.

To analyse the influence of the aperture size on the image quality we dealt first with a case when the object was placed practically on the axis ($x_0 = 0$).

For each aperture size the calculations were performed for three distances between the object points; the resulting curves are presented in Fig. 5. For comparison the values of the resolution limit for aberration-free imaging, obtained according to the Sparrow criterion, are given in this figure. It can be also noticed that for the aperture smaller than 10 mm the influence of aberrations is unno-

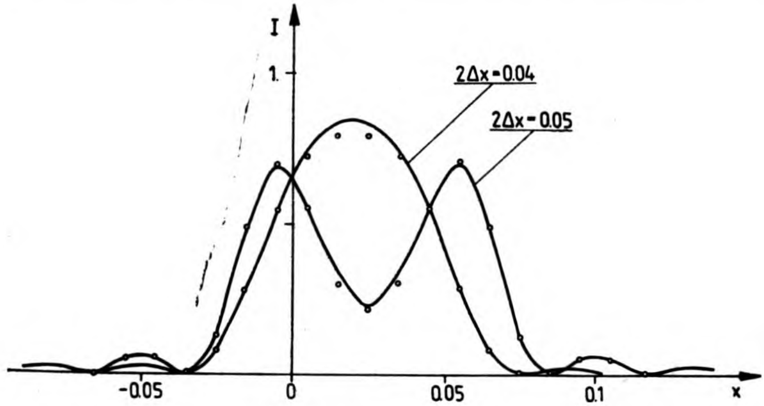

Fig. 3. Theoretical and numerically calculated light intensity distributions in an aberration-free image of a two-point object

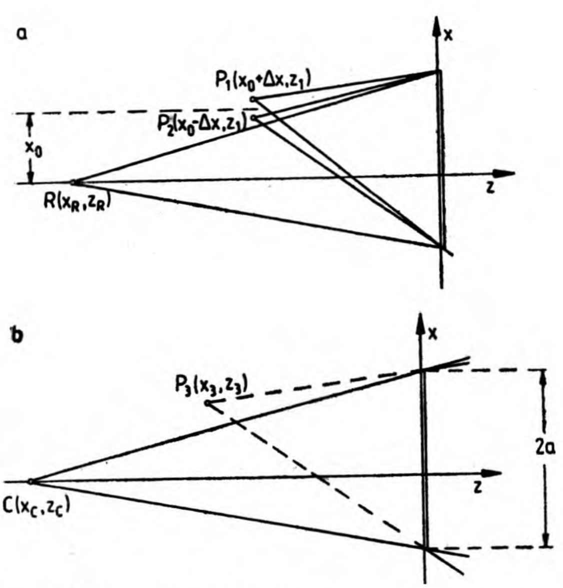

Fig. 4. Geometry of hologram recording (a) and image reconstruction (b) in the investigated case of aberrated imaging:
$x_1 = x_0 + \Delta x$, $x_2 = x_0 - \Delta x$, $x_R = 0$, $x_C = 0$
$z_1 = -100$ mm, $z_2 = -100$ mm, $z_R = -200$ mm, $z_C = -300$ mm,
$m = \mu = 1$, $\lambda_2 = 0.0006328$ mm, $z_3 = -120$ mm

ticeable, it appears only when the aperture width reaches 15 mm and is considerable above this value. It is even doubtful when the images of two points may be admitted to be resolved.

Then we investigated the influence of the field angle on the imaging quality. Constant aperture width equal to 5 mm was assumed, and the light intensity distribution in the image of the two-point object was calculated for two values

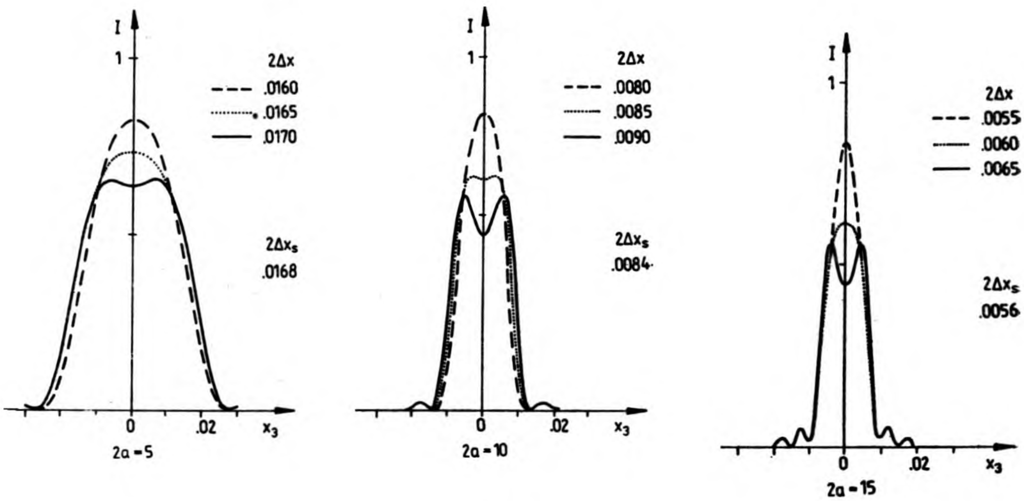

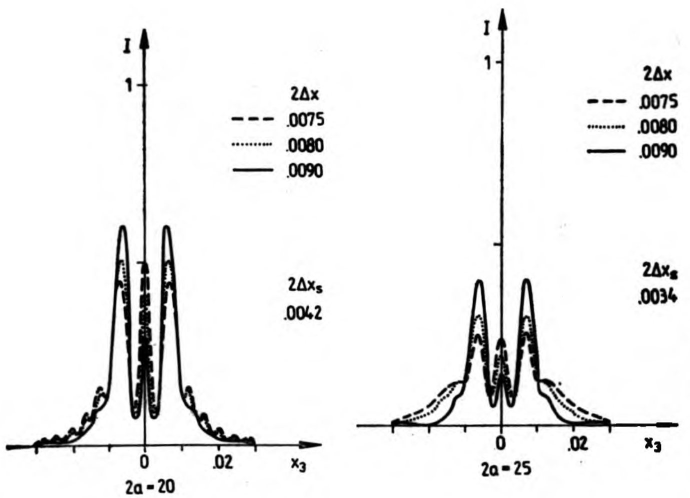

Fig. 5. Light intensity distribution in the aberrated image of a two-point object ($x_0 = 0$) for three different distances between object points and different apertures ($2\Delta x_s$ denotes the Sparrow resolution limit)

of the field, i.e., for 10 mm and 20 mm. The results are presented in Figs. 6 and 7. For the field $x_0 = 10$ mm it can be seen that a visible resolution between the two image points occurs for the distance between object points as small as $2\Delta x = 0.008$ mm. It is unexpected as this distance is smaller than the appropriate resolution limit according to Sparrow criterion. It can be seen, however, that for slightly greater distance the points are unresolved again. Only if the

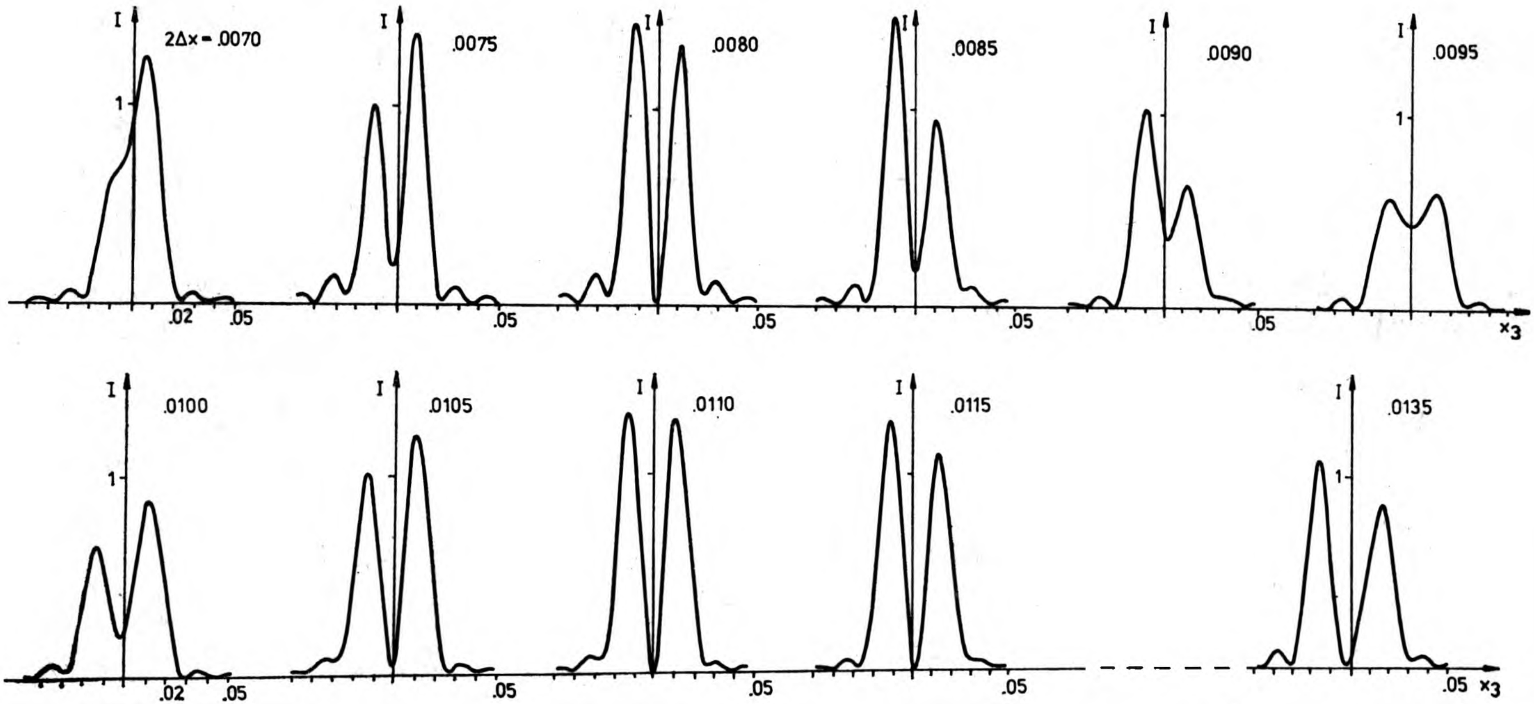

Fig. 6. Light intensity distribution in the aberrated image of a two-point object for different distances $2\Delta x$ between object points and for aperture $2a = 5$ and field $x_0 = 10$ mm

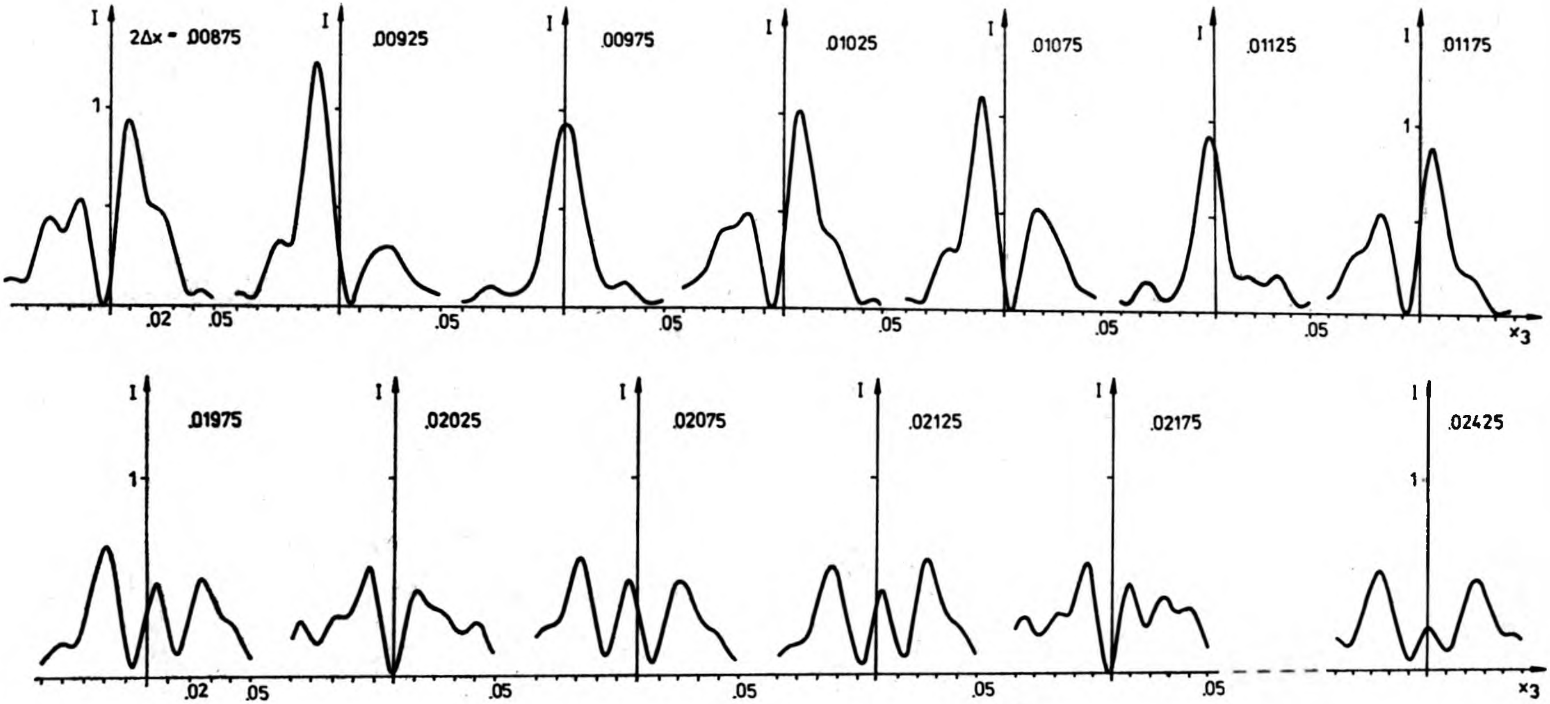

Fig. 7. Light intensity distribution in the aberrated image of a two-point object for different distances $2\Delta x$ between object points and for aperture $2a = 5$ and field $x_0 = 20$ mm

distance between them is greater than 0.01 mm the points in the image are still distinguished. The same effect is even more noticeable for the field equal to 20 mm. For the first time the image points become resolved if their distance is 0.00875 mm; it seems, however, that only for $2\Delta x$ greater than 0.02175 the points can be treated as being constantly resolved. The prior region is called by the authors *false resolution*.

As it was already stated for the case of the coherent illumination, the opinion about the imaging quality based on the analysis of the image of one- or even two-point objects should not be generalized for the case of extended objects. The investigation of the holographic imaging quality for the extended objects will be the subject of our next paper being now prepared.

References

[1] Champagne E. B., J. Opt. Soc. Am. **57** (1967), 51.
[2] Miles J. F., Optica Acta **20** (1973), 19.
[3] Born M., Wolf E., *Principles of optics*, Pergamon Press, 1964.
[4] Nowak J., Zając M., Optica Applicata **12** (1982), 353.
[5] Nowak J., Zając M., Optica Acta **30** (1983), 1749.

Received December 30, 1983

Численное исследование двухточечного распределения в голографическом отображении

В статье представлен численный алгоритм, позволяющий рассчитать распределение интенсивности света в голографическом изображении двухточечного предмета. После испытания точности этот алгоритм применялся для оценки изображений двухпточечных предметов, полученных путем голографического отображения с аберрациямн. Полученные результаты полезны для анализа влияния аберрации на двухточеченое распределение в зависимости от поля и апертуры голограммы.